[Article ID] 1003－6326(2002)06－1180－07

Photoelectrocatalytic properties and reactivity of Ti/Au-TiO_2 mesh electrodes①

LI Fang-bai(李芳柏)[1, 2], LI Xin-jun(李新军)[1], LI Xiang-zhong(李湘中)[3], HOU Mei-fang(侯梅芳)[2]
(1. Guangzhou Institute of Energy Conversion, Chinese Academy of Sciences, Guangzhou 510070, China;
2. Guangdong Key Laboratory of Agricultural Environment Pollution Integrated Control, Guangdong Institute of Eco-Environment and Soil Science, Guangzhou 510650, China;
3. Department of Civil and Structural Engineering, Hong Kong Polytechnic University, Kowloon, Hong Kong, China)

[Abstract] A kind of photoelectrode was innovated by anodising titanium mesh in H_2SO_4 solution and photo-reduced in $HAuCl_4$ solution and named Ti/Au-TiO_2 mesh electrode. The structural and surface morphology of the Ti/Au-TiO_2 mesh was examined by X-ray diffraction, laser Raman spectra, scanning electronic microscopy(SEM) and X-ray photoelectron spectroscopy respectively. The results indicate that its crystal structure, morphology and the size of pore are affected greatly by gold deposition. XPS measurement shows that the valence band of Ti/TiO_2 has two peaks: a wide one at 4.97 eV and a narrow one at 6.61 eV, which correspond mainly to π(nonbonding) and σ(bonding) O 2p orbitals. The emission intensity of O 2p orbitals becomes stronger and the width of the valence band increases with the increase of Au content. And the emission of nonbonding shifts toward lower binding energy and that of bonding O 2p orbitals shifts toward higher binding energy. The photoelectrocatalytic (PEC) oxidation of humic acid(HA) was investigated in terms of TOC. The PEC oxidation efficiency of Ti/Au-TiO_2 mesh with optimal content of gold is higher than that of Ti/TiO_2 mesh. It is suggested that the recombination of electrons and holes is hindered owing to gold deposition. The investigation shows that PEC oxidation is a convenient way to mineralize organic matter for water treatment.

[Key words] photoelectrocatalytic oxidation; water treatment; humic acid; mesh electrode; gold
[CLC number] TB 39 [Document code] A

1 INTRODUCTION

It has been confirmed that the quality of raw water in Guangzhou was deteriorating during the last few years, owing to the rapid industrialization in the region. The main pollutants in the raw water include organics (such as humic acid) and pathogens. To ensure the drinking water quality, the local water supply treatment works have to raise the chlorine dosage in the disinfection processes. However, higher dosage of chlorine results in both a higher chlorine residual concentration and also a higher trihalomethanes (THMs) concentration in product water. The presence of humic acids (HA) has been a problem in the water industry because of their water-solubility, wide range of distribution in molecular mass and size, and their non-biodegradability. It has been confirmed that humic substances play a role as precursors of chlorinated by-product (DBPs) in chlorination processes[1, 2]. It is essential to seek for new ways for water treatment.

Titanium dioxide (TiO_2)-based photo-catalysis has been the focus of numerous investigations in recent years, particularly owing to its application for the complete mineralisation of undesirable organic contaminants to CO_2, H_2O and inorganic constituents[3]. Some papers reported that humic substances could be effectively degraded in TiO_2 suspension system UV irradiation[4~6]. However, it has been also known that this type of photo-oxidation has two typical drawbacks, i.e., difficulty to separate TiO_2 particles from its aqueous suspension and low quantum yield (less than 10%, generally)[7]. To solve the problem of TiO_2 particle separation from wastewater, many researchers were trying to immobilize TiO_2 film on solid carriers such as sand, glass media or resins by coating, soaking, precipitating or spanning methods[8]. However while these immobilized TiO_2 photo-oxidation processes made the TiO_2 separation from water phase much easier, they did not improve its low quantum efficiency very much in photo-oxidation reaction.

Recently, a number of studies demonstrated that photoelectrocatalytic (PEC) oxidation process achieved a

① [Foundation item] Project(010151) supported by Guangdong Natural Science Foundation; Project(C31507) supported by Guangdong Scientific and Technological development; Project(010873) supported by Guangdong Natural Science Foundation
[Received date] 2002－05－14; [Accepted date] 2002－8－08

higher efficiency by applying an electrical bias between a working electrode and a counter electrode for organic degradation, which can prevent carrier charge recombination and result in an extension of the active holes lifetime[9, 10]. In their studies, the photo-anodes were prepared by coating TiO_2 on a conducting glass initially covered by an indium tin oxide. It was found that electron mass transfer between TiO_2 films and supporting carriers was not very efficient owing to poor connection between the two materials. Recently, we successfully prepared an innovative Ti/TiO_2 mesh photoelectrode by anodising a TiO_2 film on titanium(Ti) mesh for PEC degradation of rose Bengal[11], rhodamine B[12], humic acid[13] and methyl orange[14, 15]. This electrode has a large surface area and its microporous surface structure achieves an excellent adsorption of substances, compared with other kinds of the immobilised TiO_2 film. And it has been proved that the PEC oxidation rate using Ti/TiO_2 mesh is higher than the photo-catalytic oxidation rate in a powder suspension solution. In order to evaluate the applicability of such Ti/TiO_2, more detail investigation is needed to seek for an available way to improve its PEC activity.

In this study, the Ti/TiO_2-mesh electrode as a new type of electrode was modified by gold deposited on the surface. Humic acid was used as a model chemical to conduct the PEC oxidation experiments using the Ti/Au-TiO_2 mesh photoelectrode. The objectives of this research are: 1) to seek for an available way for water treatment and to enhance the PEC reactivity of Ti/TiO_2 mesh by surface modification; 2) to investigate the influence of gold on the crystal structure, surface morphology, chemical and electronic structure of the Ti/TiO_2-mesh electrode.

2 EXPERIMENTAL

2.1 Materials

Titanium mesh(purity > 99.6%, nominal aperture 0.19 mm, wire diameter 0.23 mm, wires/inch 60 × 60, open area 20%, twill weave) was purchased from Goodfellow Cambridge Limited. Commercially available HA was supplied from Fluka with an ash content of about 20%. All other chemicals were used with AR grade.

2.2 Preparation of Ti/TiO_2 and Ti/Au-TiO_2 mesh electrode

A large piece of raw titanium mesh was cut into small rectangle pieces of 50 mm × 10 mm × 0.5 mm, which was then cleaned with alcohol and acetone solution successively. The treated Ti mesh and a copper plate with the same size were submerged in 0.5 mol/L H_2SO_4 solution and an electrical current was applied by using a laboratory-made DC power supply. The anodisation process was conducted in two stages, in which the galvanostatic anodisation with a constant current density(0.110 A/m^2) was first performed until a designated anode-to-cathode voltage(160 V) was reached. Then the constant voltage was maintained until the end of anodisation, while the current was decreasing gradually. The freshly generated TiO_2-mesh electrode was then rinsed by distilled water and dried in an oven at 378 K for 2 h. The preparation method had been described by Li et al[11]. The photo-electrode was noted as 160 V-mesh (or No gold).

The anodized Ti/TiO_2 mesh electrode is modified by the photo-reduction method to deposit gold. The Ti/TiO_2 mesh is placed in a mixture of solution containing the required concentration of tetrachloroauric acid and 0.1 mol/L methanol. The solution was irradiated with a high-pressure mercury lamp. The irradiation lasted 20, 40, 60, 80 min respectively. The produced Ti/Au-TiO_2 mesh electrode is washed repeatedly with double distilled water and dried at 378 K for 2 h. The gold concentration on the surface of Ti/TiO_2 mesh was detected by XPS. The gold concentration on the surface of four pieces of Ti/Au-TiO_2 mesh electrodes was 2.01% (mole fraction), 3.34%, 6.71% and 17.3% respectively. And they were noted as Au1# -mesh, Au2# -mesh, Au3# -mesh and Au4# -mesh respectively.

2.3 Characterization of Ti/Au-TiO_2-mesh electrode

To determine the crystal phase composition of Ti/Au-TiO_2 mesh, X-ray diffraction(XRD) measurements was performed at room temperature with a Philips PW3710 diffractometer using Cu K_α radiation(λ_1 = 0.154 060 nm; λ_2 = 0.154 439 nm); accelerating voltage was 40 kV, and emission current was 30 mA. Laser Raman spectroscopy was used to determine the crystal pattern of TiO_2(anatase and rutile) on the mesh electrode. At room temperature, Raman spectra were excited by 514.5 nm laser line from a CW argon laser(Coherent Innva 70). The laser power was kept at 250 mW to avoid laser annealing of the samples. A 55 mm f/1.8 lens was used for collecting the scattering light which was dispersed and detected using a double grating monochromator(Spex 1403) equipped with a cooled photomultiplier tube(PMT, Hamamatus R943-2). All spectra were recorded in a small angle scattering geometry. The resolution obtained was expected to be as good as 1 cm^{-1}. Scanning Electron Microscopy(SEM) (Leica Stereoscan

400i Series) was used to study the surface morphology, average pore size and pores distribution. High tension was selected at 15 kV. X-ray photoelectron spectroscopy (XPS) was recorded with a PHI Quantum ESCA Microprobe System, using the Mg K_α line of a 250 W Mg X-ray tube as the radiation source with the energy of 1 253.6 eV, 16 mA × 12.5 kV. The working pressure was less than 1×10^{-8} N/m^2. As an internal reference for the absolute binding energies, the C1s peak of hydrocarbon contamination was used. The fitting XPS curves were analyzed by use of Multipak 6.0 A.

2.4 Photo-reactor and PEC oxidation of HA

PEC oxidation experiment was performed in a batch photo-reactor system, which consisted of a cylindrical borosilicon glass reactor with an effective volume of 165 mL, a 125 W high-pressure mercury lamp, a potentiostat (ISO-TECH 1PS 1810H) and electrodes. The 125 W high-pressure mercury lamp (Institute of Electric Light Source, Beijing) was positioned inside a cylindrical Pyrex vessel surrounded by a circulating water jacket (Pyrex) to cool the lamp. In the photo-reactor, two electrodes of Ti/Au-TiO_2-mesh electrode as anode and copper plate electrode (50 mm × 10 mm) as cathode were placed oppositely and connected with the potentiostat. 165 mL of HA solution was irradiated under constant aerating. At given irradiation time intervals, samples of the suspension were taken and analyzed.

In the study, a set of tests was carried out by using the Ti/Au-TiO_2-mesh electrode to investigate the effect of gold on PEC efficiency. The TOC representing the PEC degradation degree of humic acid was determined with a Shimadzu TOC-5000A TOC analyzer. The light intensity was measured by using a Black-Ray UV meter (UVP Inc, Model No. J 221).

3 RESULTS AND DISCUSSION

3.1 Crystal structural analyses of Ti/Au-TiO_2-mesh electrodes

The crystal phase composition of the Ti/Au-TiO_2-mesh electrodes was examined by XRD. Their diffractions are shown in Fig. 1, where the peaks representing anatase and rutile forms of TiO_2 are labelled with A and R respectively. For 160 V-mesh, rutile phase presents at 27.405° (110), 36.105°, 41.310° and 56.685°. The 101 peak is very weak. For Ti/Au-TiO_2 mesh, the intensity of anatase and rutile peaks is influenced by gold and increases with the increase of the gold content. For all Ti/Au-TiO_2 mesh, 101 peak and 110 peak present significantly, compared with 160 V-mesh.

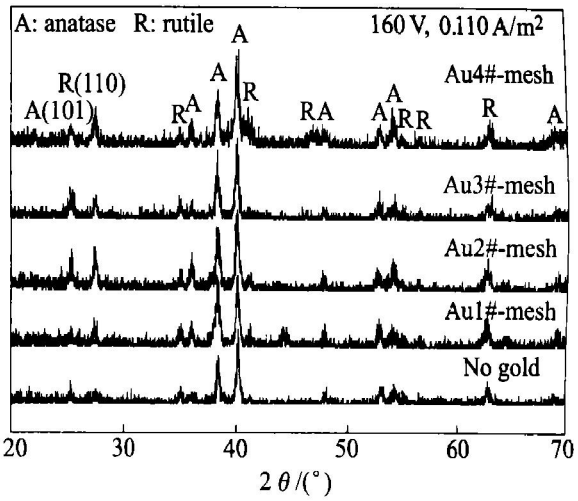

Fig. 1 X-ray diffraction results of Ti/Au-TiO_2 mesh electrodes

In this paper, the effect of gold deposition on the formation of crystal phase might be investigated in detail by means of laser Raman spectra shown in Fig. 2, in which the peaks representing the anatase and rutile forms of TiO_2 are labelled with A and R respectively. For 160 V-mesh, the anatase peaks are located at 102, 141, 222, 352, 519 and 638 cm^{-1} while that of rutile are observed at 439 and 625 cm^{-1}. The strongest peak of anatase occurs at around 141 cm^{-1} with a narrow line shape for 160 V-mesh. For all samples, the LR spectra also indicate that the anatase phase of TiO_2 is dominant. For Au1# -mesh and Au2# -mesh, the intensity of the phonon peak for anatase at 222 cm^{-1} increases significantly whereas those of other peaks decrease slightly. For Au3# -mesh and Au4# -mesh, the intensity of the phonon peak for anatase decreases significantly and that of rutile does not appear, with the increase of the gold content. The surface morphology of Ti/Au-TiO_2 mesh as shown in Fig. 3 shows that gold clusters cover on the surface of Ti/Au-TiO_2 mesh.

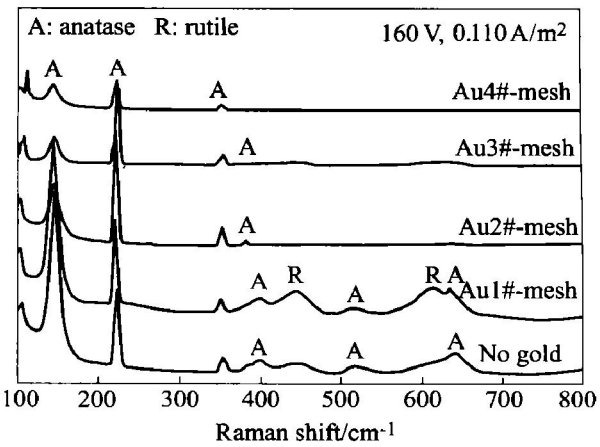

Fig. 2 Laser Raman spectroscopy of Ti/Au-TiO_2 mesh electrodes

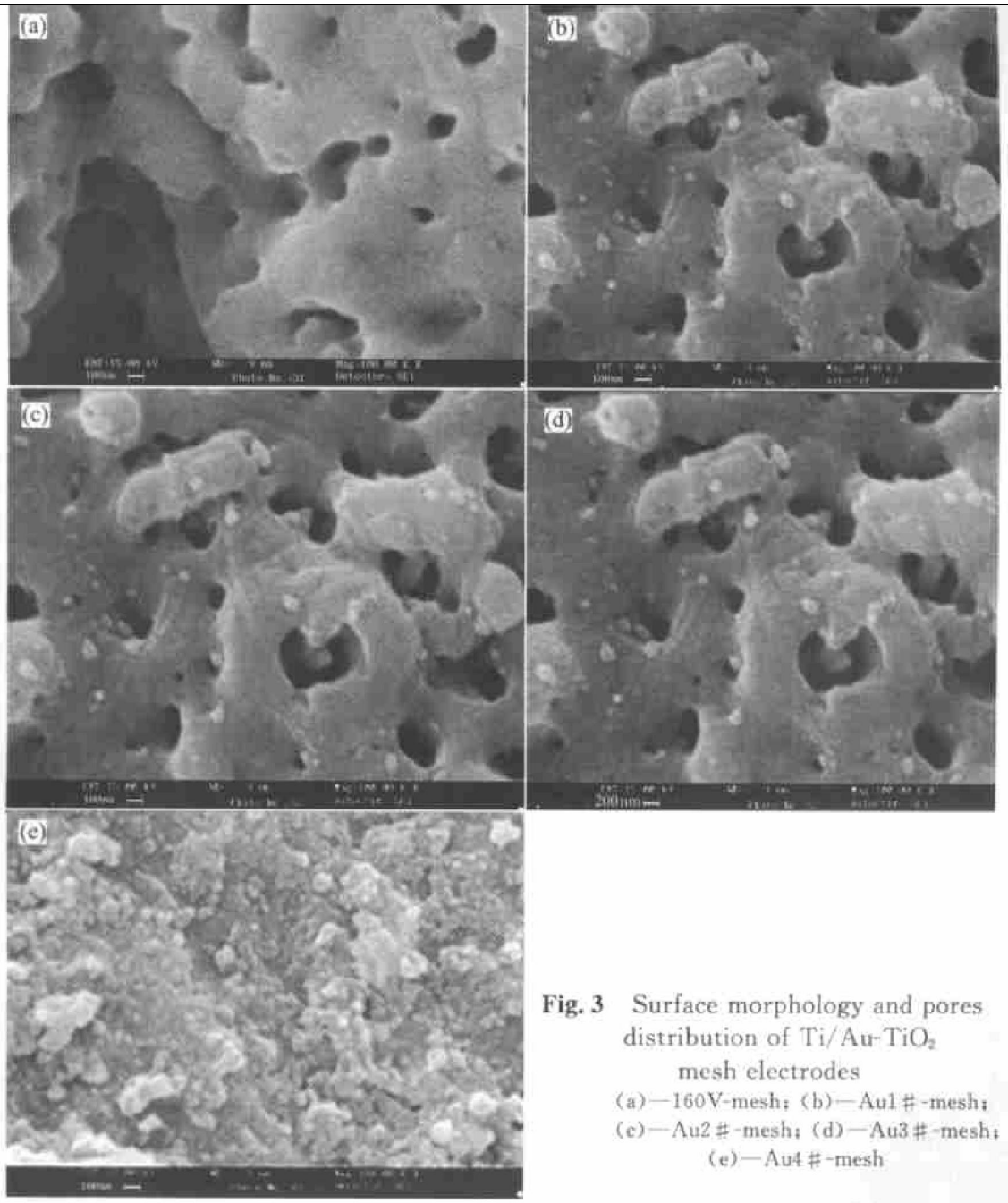

Fig. 3 Surface morphology and pores distribution of Ti/Au-TiO_2 mesh electrodes
(a)—160V-mesh; (b)—Au1#-mesh; (c)—Au2#-mesh; (d)—Au3#-mesh; (e)—Au4#-mesh

3.2 Surface morphology and pore distribution of Ti/Au-TiO_2 mesh electrodes

The morphology of the Ti/Au-TiO_2-mesh electrodes is examined by means of SEM and their SEM photos are shown in Figs. 3(a) ~ 3(e). It is found that the surface of Ti/Au-TiO_2 film is meiroporous and rougher. The surface morphology of Ti/Au-TiO_2 mesh is influenced by the gold deposited on the surface, as shown in Figs. 3(b) ~ 3(e). For Au1#-mesh, the size of gold clusters is about 15 ~ 30 nm and only a small part of surface is covered. However, for Au4#-mesh, the size of gold clusters increases significantly and is about 15 ~ 70 nm. And the pores are almost filled up.

3.3 Electronic structure of Ti/Au-TiO_2 mesh electrodes

XPS analyses were carried out to determine the chemical and electronic structure of mesh surface and to disclose the mechanism of the variation of PEC properties and PEC reactivity. The Ti 2p, O 1s, Au 4f and valence band XPS spectra of all mesh fitted by Multipak 6.0A software are listed in Table 1, Table 2 and shown in Figs. 4 ~ 7.

The O 1s spectra of Ti/Au-TiO_2 mesh are shown in Fig. 4, and the binding energy of O 1s is listed in Table 1. Sanjinés et al[16] reported that the O 1s spectra of reduced samples were proposed to consist of three components attributed to the oxide component(530.0 eV), hydroxyl groups or defective oxides(531.5 ±0.5 eV), and oxygen chemisorbed or adsorbed water(533 ±1 eV). In our investigation, the O 1s XPS spectra of Ti/Au-TiO_2 mesh shows a two-band structure. The peak at 529.59 ~ 529.83 eV is in agreement with O 1s electron binding energy for TiO_2 molecular with a shift toward to higher binding energy owing to gold deposition. Another O 1s band at 531 ~ 532 eV may be attributed to hydroxyl

Table 1 Molar percentage of gold and binding energy of O 1s, Ti 2p and Au 4f of Ti/Au-TiO_2 mesh

Mesh	x(Au)/%	Binding energy/eV				
		O 1s	Ti $2p_{1/2}$	Ti $2p_{3/2}$	Au $4f_{5/2}$	Au $4f_{7/2}$
160 V-mesh	0	529.59	464.01	458.27		
Au1# -mesh	2.2	529.63	464.23	458.35	87.62	83.94
Au2# -mesh	3.4	529.81	464.44	458.54	87.49	83.86
Au3# -mesh	6.7	529.83	464.54	458.59	87.39	83.71
Au4# -mesh	17.3	529.94	464.37	458.62	87.30	83.63

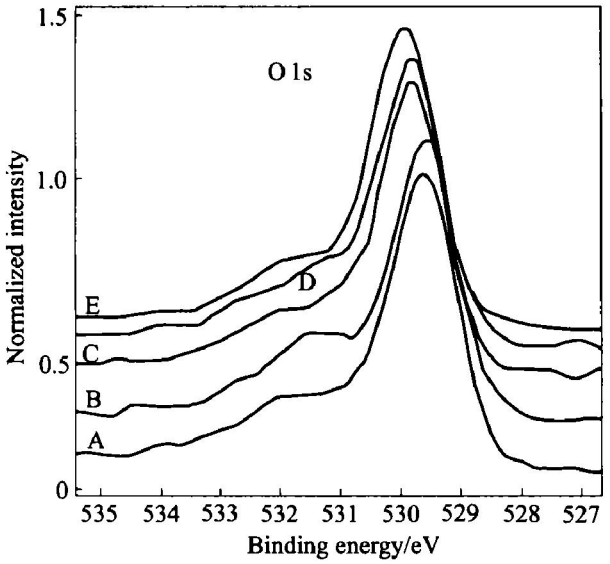

Fig. 4 O 1s XPS curves of Ti/Au-TiO_2 mesh fitted by Multipak 6.0 A
(Remarks A, B, C, D, E represent Ti/TiO_2 mesh, Au 1#, Au 2#, Au 3#, Au 4# respectively, the same as following figures)

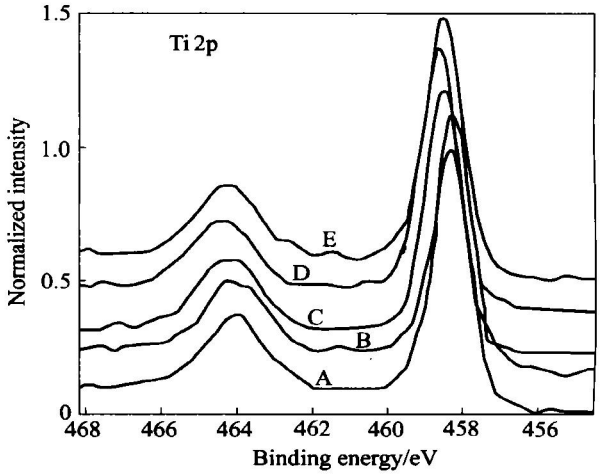

Fig. 5 Ti 2p XPS curves of Ti/Au-TiO_2 mesh fitted by Multipak 6.0 A

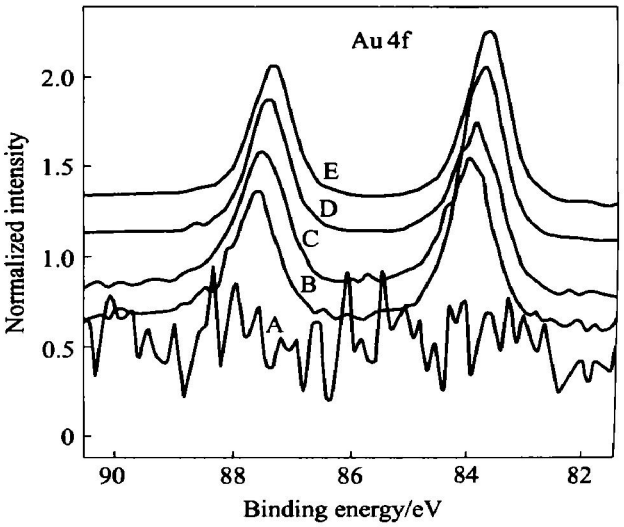

Fig. 6 Au 4f XPS curves of Ti/Au-TiO_2 mesh fitted by Multipak 6.0 A

groups. The intensities of Ti 2p and O 1s XPS peaks decrease with the increase of gold cluster covered on the surface of Ti/Au-TiO_2 mesh.

The Ti $2p_{3/2}$ peak for Ti/Au-TiO_2 mesh is narrow with slight asymmetry and has a binding energy of 458.27 ~ 458.62 eV, attributed to Ti^{4+}, as shown in Fig. 5. In the meantime, the Ti $2p_{1/2}$ peak is weaker and wider with a core level of 464.01~ 464.54 eV. The results show that the binding energies of Ti $2p_{3/2}$ and Ti $2p_{1/2}$ increase slightly owing to gold deposition. The intensity of Ti 2p XPS peaks decreases with the increase of gold cluster covered on the surface of Ti/Au-TiO_2 mesh.

In Fig. 6, the Au 4f peak of Ti/Au-TiO_2 mesh consists of two peaks, corresponding to Au $4f_{2/5}$ and Au $4f_{2/7}$ respectively. The binding energies of Au $4f_{2/5}$ and Au $4f_{2/7}$ slightly decrease with the increase of photo-reduction time and gold content. Ti/Au-TiO_2 mesh was prepared by photo-reduction. At first, $AuCl_4^-$ was absorbed on the surface of Ti/TiO_2 mesh, then reduced into $AuCl_2^-$ and Au^0 or $(Au^0)_m$ at the end. Some nanoparticles of metals such as Au have strong optical absorption by surface plasmon resonance in the visible light wavelength[17]. Metallic gold deposited on the surface of TiO_2 can significantly absorb visible light.

The valence-band spectra of Ti/TiO_2 mesh and Ti/Pt-TiO_2 mesh are shown in Fig. 7. The valence band of Ti/TiO_2 have two peaks: a board one at 4.97 eV and a narrow one at 6.61 eV, which correspond mainly to π (nonbonding) and σ(bonding) O 2p orbitals, as listed

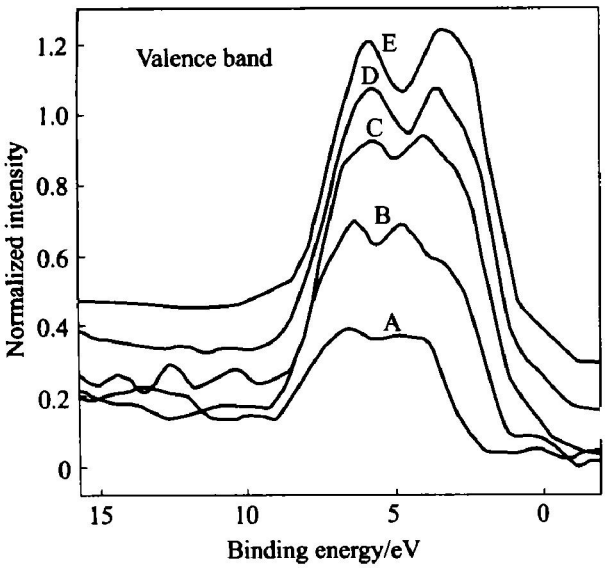

Fig. 7 Valence band spectra of XPS curves of Ti/Au-TiO_2 mesh fitted by Multipak 6.0 A

in Table 2. It deserves noting that the intensity emissions of O 2p nonbonding orbitals located at 4.84, 4.16, 3.66, 3.39 eV respectively for Au1# , Au2# , Au3# , Au4# , and became stronger and the width of the valence band and the emission intensity increased with the increase of Au content on the surface of mesh. In the meantime, the emission peaks of O 2p bonding orbitals are located at 5.56, 5.76, 5.89, 5.77 eV respectively. Compared to literature, Sanjinés et al[16] reported that the valence band of anatase TiO_2 was confined to binding energy between 3 and 9 eV, relative to Fermi level(E_F) showing two peaks: a board one at 6 eV and a narrow one at 8 eV; and a significant electron emission near the Fermi level indicated that Ti^{3+} defect states were located in the band gap, 0.7~ 0.9 eV below E_F. In our investigation, what was different from the XRD diagram of powder, the strongest peak of anatase for all mesh presented at 40.295°, not at 25.405° attributable to 101 peak. The intensities of anatase and rutile peaks increase with the increase of the gold content. The differences of XRD peaks position and intensity lead to the change of the valence band, band gap and surface states.

Table 2 Peaks of valence band spectra and hydroxyl group(eV)

Catalyst	Peak 1	Peak 2
TiO_2	4.97	6.61
Au1#	4.84	6.56
Au2#	4.16	5.76
Au3#	3.66	5.89
Au4#	3.39	5.77

3.4 PEC reactivity of Ti/Au-TiO_2 mesh electrodes

To investigate the effect of gold deposition on the PEC reactivity of Ti/Au-TiO_2 mesh, a set of tests were conducted by using 160 V-mesh, Au1# -mesh, Au2# -mesh, Au3# -mesh and Au4# -mesh with the same light intensity of 4.38 $mW \cdot cm^{-2}$ and without electrical bias voltage. The initial concentration of HA solution was 10 mg/L. The results show that the TOC removal would be greatly promoted when optimal gold was deposited on the surface of Ti/Au-TiO_2 mesh electrode as shown in Fig. 8. For 4 Ti/Au-TiO_2 mesh electrodes (Au1# , Au2# , Au3# , Au4#), the first-order kinetic constants were 0.014 9, 0.025 6, 0.018 8, 0.007 8 min^{-1} respectively. And that of Ti/TiO_2 mesh was 0.010 4 min^{-1}. When the content of gold was 3.34%, the PEC efficiency was the highest, and the higher content of gold on the surface of Ti/TiO_2 mesh was detrimental to raise the PEC efficiency.

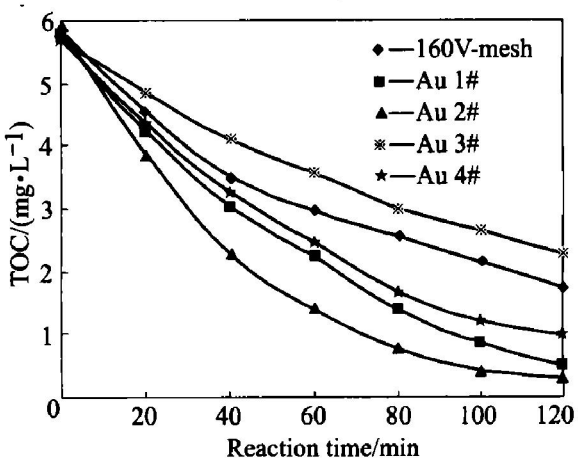

Fig. 8 TOC removal of HA solution with reaction time at pH= 3.01

4 DISCUSSION

The PEC mechanism on the Ti/TiO_2 working electrode and the copper counter electrode has been proposed in detail in our previous works[18]. For Ti/Au-TiO_2 mesh, the excited electrons from valence band to conduction band migrated to gold clusters, then migrated to O_2 moleculae absorbed on the surface of gold. Au on TiO_2 surface produces the highest Schottky barrier among the metals facilitating the electron capture[19]. And O_2^- is an active species to oxidise the HA.

$$Ti/Au-TiO_2 \rightarrow ((Ti/Au-TiO_2)e_{cb}^-)_{WE} + ((Ti/Au-TiO_2)-h_{vb}^+)_{WE} \quad (1)$$

$$((Ti/Au-TiO_2)-e_{cb}^-)_{WE} + (O_2)_s \rightarrow ((Ti/Au-TiO_2)-(O_2^-)_s)_{WE} \quad (2)$$

$$(O_2^-)_s + HA \rightarrow \cdots \rightarrow CO_2 + \text{inorganic species} \quad (3)$$

In addition to the redox reactions on the working and counter electrodes, there is an important reaction on the working electrode. The reaction is the recombination of excited electrons and holes.

$$((Ti/TiO_2)-e^-_{cb})_{WE}+((Ti/TiO_2)-h^+_{vb})_{WE}\rightarrow heat \quad (4)$$

In fact, the charge recombination process was a significant factor in decreasing the PEC efficiency on TiO_2 film[20, 21]. Therefore, reducing the recombination of electrons and holes is essential to promote PEC efficiency. In our investigation, optimal content of gold deposited on the surface of Ti/TiO_2 mesh can improve the PEC rate. Many investigations show that gold deposited on the TiO_2 surface could promote the excited electron transfer, immigration and separation and hinder the recombination of electrons and holes[19, 21, 22].

5 CONCLUSIONS

1) Photoelectrocatalysis using a new type of photoelectrode, Ti/Au-TiO_2-mesh electrode that was successfully innovated by anodizing Ti Mesh in 0.5 mol/L H_2SO_4 solutions and by photoreduction, can be used to degrade efficiently HA. TOC in HA solution was removed rapidly after irradiation for 120 min.

2) The XRD and laser Raman spectra indicated that the anatase form of TiO_2 was dominant on the surface of the electrode, and the intensities of anatase and rutile XRD peaks all increased with the increase of gold on the mesh surface, and the intensity of laser Raman peaks decreased owing to a higher gold deposition.

3) SEM measurement showed that gold cluster covered on the surface of Ti/Pt-TiO_2 mesh and filled up the pore of the mesh. XPS measurement showed that the binding energy of O 1s and Ti 2p increased slightly and that of Au $4f_{2/7}$ and Au $4f_{2/5}$ decreased slightly owing to gold deposition. The PEC activity of 160 V-mesh was promoted when an optimal content of gold was deposited.

[REFERENCES]

[1] Singer P C. Humic substances as precursors for potentially harmful disinfection by-products[J]. Wat Sci Tech, 1999, 40(9), 25-30.

[2] LI J W, YU Z B, GAO M, et al. Effect of ultraviolet irradiation on the characteristics and trihalomethanes formation potential of humic acid[J]. Wat Res, 1996, 30(2): 347-350.

[3] Hoffmann M R, Martin S T, Choi W Y, et al. Environmental applications of semiconductor photocatalysis[J]. Chem Rev, 1995, 95(1): 69-96.

[4] Bekbölet M, Ozkosemen G. A preliminary investigation on the photocatalytic degradation of a model humic acid[J]. Wat Sci Tech, 1996, 33(6): 189-194.

[5] Bekbölet M, Balcioglu I. Photocatalytic degradation kinetics of humic acid in aqueous TiO_2 dispersions: the influence of hydrogen peroxide and bicarbonate ion[J]. Wat Sci Tech, 1996, 34(9): 73-80.

[6] Eggins B R, Palmer F L, Byrne J A. Photocatalytic treatment of humic substances in drinking water[J]. Wat Res, 1997, 31(5): 1223-1226.

[7] Choi W Y, Termin A, Hoffmann M R. Effects of metal-ion dopants on the photocatalytic reactivity of quantum-sized TiO_2 particles[J]. Angew Chem Int Edit, 1994, 33(10): 1091.

[8] Bideau M, Claudel B, Dubien C, et al. On the "immobilization" of titanium dioxide in the photocatalytic oxidation of spent water[J]. J Photochem Photobio A, 1995, 91: 137-144.

[9] Kesselman J M, Lewis N S, Hoffmann M R Environ. Photoelectrochemical degradation of 4-chlorocatechol at TiO_2 electrodes: Comparison between sorption and photoreactivity[J]. Sci Technol, 1997, 31(8): 2298-2305.

[10] Vinodgopal K, Hotchandani S, Kamat P V. Electrochemically assisted photocatalysis-TiO_2 particulate film electrodes for photocatalytic degradation of 4-chlorphenol[J]. J Phys Chem-US, 1993, 97(35): 9040-9044.

[11] LI X Z, LIU H L, YUE P T, et al. Photoelectrocatalytic oxidation of rose bengal in aqueous solution using a Ti/TiO_2 mesh electrode[J]. Environ Sci Technol, 2000, 34: 4401-4406.

[12] LI X Z, LIU H L, LI F B, et al. Photoelectrocatalytic oxidation of rhodamine B in aqueous solution using Ti/TiO_2 mesh photoelectrodes[J]. J Environ Sci Health, A. 2002, 37(1), 55-69.

[13] LI X Z, LI F B, FAN C M, et al. Photo-electro-catalytic degradation of humic acid in aqueous solution using a Ti/TiO_2 photo-electrode[J]. Water Research, 2002, 36(9), 2215-2224.

[14] LI Fang-bai, LI Xiang-zhong, KANG Yue-hui, et al. An innovative Ti/TiO_2 mesh photo-electrode for methyl orange photo-electro-catalytic degradation[J]. J Environ Sci Health, A. 2002, 37(4), 623-640.

[15] LI Fang-bai, WANG Liang-yan, LI Xin-jun, et al. Preparation and properties of innovative Ti/TiO_2 mesh photoelectrode for methyl orange photoelectrocatalytic oxidation[J]. The Chinese Journal of Nonferrous Metals, 2001, 11(6): 977-981.

[16] Sanjinés R, Tang H, Berge H, et al. Electronic structure of anatase TiO_2 oxide[J]. J Appl Phys, 1994, 75: 2945.

[17] Yonezawa T, Matsune H, Kunitake T. Layered nanocomposite of close-packed gold nanoparticle and TiO_2 gel layers[J]. Chem Mater, 1999, 11: 33-35.

[18] LI X Z, LI F B. Surface characterization and photocatalytic reactivity of innovative Ti/TiO_2 and Ti/Pt-TiO_2 mesh photoelectrodes[J]. J Appl Electrochem, 2002, 32, 203-210.

[19] Linsebigler A, Lu G Q, Yates J T. Photocatalysis on the TiO_2 surface: principal, mechanisms and selected results[J]. Chem Rev, 1995, 95, 735-760.

[20] Rajeshwar K. Photoelectrochemistry and the environment[J]. Journal of applied electrochemistry, 1995, 25: 1067-1082.

[21] Tryk D A, Fujishima A, Honda K. Recent topics in photoelectrochemistry: achievements and future prospects[J]. Electrochimica Acta, 2000, 45: 2363-2376.

[22] WANG C Y, LIU C Y, ZHENG X, et al. The surface chemistry of hybrid nanometer-sized particles 1. photochemical deposition of gold on ultrafine TiO_2 particles[J]. Colloids and Surfaces A, 1998, 131: 271-280.

(Edited by PENG Chao-qun)